0026-895X/10/7704-517–528
MOLECULAR PHARMACOLOGY
U.S. Government work not protected by U.S. copyright
Mol Pharmacol 77:517–528, 2010

Vol. 77, No. 4
62539/3569035
Printed in U.S.A.

Detergent-Resistant Microdomains Determine the Localization of σ-1 Receptors to the Endoplasmic Reticulum-Mitochondria Junction[S]

Teruo Hayashi and Michiko Fujimoto

Cellular Pathobiology Section, Cellular Neurobiology Research Branch, Intramural Research Program, National Institute on Drug Abuse, National Institutes of Health, Department of Health and Human Services, Baltimore, Maryland

Received November 17, 2009; accepted January 6, 2010

ABSTRACT

σ-1 receptors (Sig-1Rs) that bind diverse synthetic and endogenous compounds have been implicated in the pathophysiology of several human diseases such as drug addiction, depression, neurodegenerative disorders, pain-related disorders, and cancer. Sig-1Rs were identified recently as novel ligand-operated molecular chaperones. Although Sig-1Rs are predominantly expressed at endoplasmic reticulum (ER) subdomains apposing mitochondria [i.e., the mitochondria-associated ER membrane (MAM)], they dynamically change the cellular distribution, thus regulating both MAM-specific and plasma membrane proteins. However, what determines the location of Sig-1R at the MAM and how the receptor translocation is initiated is unknown. Here we report that the detergent-resistant membranes (DRMs) play an important role in anchoring Sig-1Rs to the MAM. The MAM, which is highly capable of accumulating ceramides, is enriched with both cholesterol and simple sphingolipids, thus forming Triton X-114-resistant DRMs. Sig-1Rs associate with MAM-derived DRMs but not with those from microsomes. A lipid overlay assay found that solubilized Sig-1Rs preferentially associate with simple sphingolipids such as ceramides. Disrupting DRMs by lowering cholesterol or inhibiting de novo synthesis of ceramides at the ER largely decreases Sig-1R at DRMs and causes translocation of Sig-1R from the MAM to ER cisternae. These findings suggest that the MAM, bearing cholesterol and ceramide-enriched microdomains at the ER, may use the microdomains to anchor Sig-1Rs to the location; thus, it serves to stage Sig-1R at ER-mitochondria junctions.

The σ receptor is believed to serve as a novel target for therapeutic drugs. Although originally proposed as a subtype of opioid receptors, a series of recent studies has confirmed that the σ receptor is a nonopioid intracellular protein involved in a variety of functions of the brain and other organs (Snyder and Largent, 1989; Hayashi and Su, 2008). There are two known subtypes: σ-1 and σ-2 (Bowen, 2000). The σ-1 receptors (Sig-1Rs) were cloned, and the structure and molecular biological functions have just begun to be unveiled (Hanner et al., 1996; Hayashi and Su, 2008). Sig-1Rs have been implicated in the pathophysiology of certain human diseases such as psychiatric disorders, neurodegenerative diseases, pain-related disorders, and cancer (Maurice et al., 2002; Matsumoto et al., 2003; Mei and Pasternak, 2007; Palmer et al., 2007). Recent evidence indicates potential neuroprotective and antidepressant-like actions for σ-1 agonists (Maurice et al., 2002). In contrast, σ-1 antagonists have been demonstrated to possess analgetic, anticancer, and anti–drug-abuse actions (Matsumoto et al., 2003; Mei and Pasternak, 2007; Palmer et al., 2007).

The Sig-1Rs are the integral membrane proteins with two transmembrane domains and a long C terminus in the lumen

This study was supported by the Intramural Research Program, National Institute on Drug Abuse, National Institutes of Health, Department of Health and Human Services.

Article, publication date, and citation information can be found at http://molpharm.aspetjournals.org.

doi:10.1124/mol.109.062539.

[S] The online version of this article (available at http://molpharm.aspetjournals.org) contains supplemental material.

ABBREVIATIONS: Sig-1R, σ-1 receptor; ANS, 8-anilinonaphthalene-1-sulfonate; BODIPY-Cer TR, *N*-((4-(4,4-difluoro-5-(2-thienyl)-4-bora-3a,4a-diaza-s-indacene-3-yl)phenoxy)acetyl)sphingosine; BSA, bovine serum albumin; CHO, Chinese hamster ovary; CHAPS, 3-[(3-cholamidopropyl) dimethylammonio]-1-propanesulfonate; CYP450R, cytochrome P450 reductase; DRM, detergent-resistant membrane; ER, endoplasmic reticulum; EYFP, enhanced yellow fluorescent protein; FB1, fumonisin B1; GFP, green fluorescent protein; GlcCer, glucosylceramide; HPTLC, high-performance thin-layer chromatography; IP3R3, type-3 inositol 1,2,5-trisphosphate receptor; MAM, mitochondria-associated endoplasmic reticulum membrane; MβC, methyl-β-cyclodextrin; NBD-Cer, 6-((*N*-(7-nitrobenz-2-oxa-1,3-diazol-4-yl)amino)hexanoyl)sphingosine; PBS, phosphate-buffered saline; PAGE, polyacrylamide gel electrophoresis; TNE, Tris-NaCl-EDTA buffer; TNC, Tris-NaCl-CHAPS buffer; Tx, Triton X-100; PDMP, (±)-*threo*-1-phenyl-2-decanoyl-amino-3-morpholino-1-propanol hydrochloride; MβC-Chol, methyl-β-cyclodextrin presaturated with cholesterol.

of the ER (Hayashi and Su, 2007). A characteristic of Sig-1Rs is their moderate to high affinity for diverse synthetic and endogenous compounds including benzomorphans, sterols, sphingosine, and trace amines (Su et al., 1988; Bowen, 2000; Fontanilla et al., 2009; Ramachandran et al., 2009). Sig-1Rs were recently identified as novel ligand-operated molecular chaperones expressed predominantly at the ER subdomain-apposing mitochondria (the mitochondria-associated ER membrane, MAM) (Hayashi and Su, 2007). Thus, Sig-1Rs are positioned to regulate the cross-talk of signals between ER and mitochondria. For example, Sig-1R chaperones stabilize the conformation of MAM-residing type-3 inositol 1,4,5-trisphosphate receptors (IP3R3), thus regulating the Ca^{2+} influx from the ER to mitochondria (Hayashi et al., 2009). On the other hand, a number of studies demonstrate that Sig-1Rs also regulate cellular events at plasma membranes, such as neurotransmitter release, neurotrophic factor signaling, and opening of voltage-gated ion channels (Aydar et al., 2002; Nuwayhid and Werling, 2003; Hayashi and Su, 2008; Herrera et al., 2008). The tonic inhibition of the potassium Kv1.4 channel by Sig-1Rs involves the physical association between Sig-1R and Kv1.4 channels (Aydar et al., 2002). Although Sig-1Rs are predominantly expressed at the MAM, the proteins are highly dynamic under certain conditions, such as glucose deprivation and ligand treatment, which promote translocation of Sig-1R from the MAM to loci close to plasma membranes (e.g., plasmalemma) (Hayashi and Su, 2003a, 2007). The phenomenon is particularly important and relevant for understanding the Sig-1R's regulatory role on both ER and plasma membrane proteins. The dynamic shift of the receptor distribution may be to switch the action site of Sig-1R from the MAM to the plasma membrane/plasmalemma (Hayashi and Su, 2008). What determines the location of Sig-1R at the MAM and how the receptor translocation is initiated/restricted, however, remain largely unknown.

Lipid rafts composed of cholesterol and sphingolipids are small-membrane domains that facilitate specificity and efficacy of signaling events by positioning involved molecules to the specific loci of the membrane (Simons and Toomre, 2000; Jacobson et al., 2007). Lipid rafts are resistant to extraction by nonionic detergents such as Triton X-100 (Tx) at 4°C; therefore, lipid rafts can be purified as detergent-resistant membranes (DRMs) by centrifugation (Simons and Toomre, 2000). We reported previously that Sig-1Rs are associated with DRM at cholesterol-rich ER subdomains (now identified as the MAM) in different types of cells (Hayashi and Su, 2003b, 2004) and that Sig-1R ligands, which can cause translocation of Sig-1R from MAM to the bulk of ER membranes, also down-regulate Sig-1R at DRMs (Hayashi and Su, 2003a,b). Because of DRMs serving as platforms to cluster signaling molecules, these findings raise a potential hypothesis that ER-specific DRMs may play a role in the targeting of Sig-1Rs at the ER-mitochondria junction. Thus, the objective of this study was to examine whether DRMs are involved in the localization of Sig-1Rs at the MAM and in the receptor translocation.

Materials and Methods

Materials and Methods. Reagents for cell culture were purchased from Invitrogen (Carlsbad, CA). Sources of antibodies included the following: anti-N-CAM was from BD Biosciences Pharmingen (San Diego, CA); anti-IP3R3 and anti-BiP were from BD Biosciences (San Jose, CA); anti-Src, anti-cytochrome P450 reductase (CYP450R), and anti-calreticulin were from Santa Cruz Biotechnology (Santa Cruz, CA); anti-ceramide was from Sigma-Aldrich (St. Louis, MO), anti-mitofusin-2 and anti-ERp57 were from Abcam Inc. (Cambridge, MA); anti-ATP synthase inhibitor and anti-cytochrome *c* oxidase subunit I were from Invitrogen; and anti-green fluorescent protein (GFP) was from Clontech (Mountain View, CA). Anti-Sig-1R antibodies were developed as described previously (Hayashi and Su, 2007). 6-((*N*-(7-nitrobenz-2-oxa-1,3-diazol-4-yl)amino)hexanoyl) sphingosine (NBD-Cer) and *N*-((4-(4,4-difluoro-5-(2-thienyl)-4-bora-3a,4a-diaza-s-indacene-3-yl)phenoxy)acetyl)sphingosine (BODIPY-Cer TR) were from Invitrogen. Chemicals and lipids were from Sigma-Aldrich or Avanti Polar Lipids (Alabaster, AL). Expression vectors for Mito-DsRed, Mito-GFP, and KDEL-DsRed were purchased from Clontech. The structures of lipids are provided in the supplemental figure.

Cell Culture. Chinese hamster ovary (CHO; American Type Culture Collection, Manassas, VA) cells were maintained in minimum essential medium-α containing 2 mM GlutaMax (Invitrogen) and 10% heat-inactivated fetal calf serum at 37°C with 5% CO_2. The vector encoding the mouse Sig-1R with an enhanced yellow fluorescent protein (EYFP)-tag on the C terminus was constructed in the pEYFP-N1 vector (Clontech) as described previously (Hayashi and Su, 2003b). CHO cell lines stably expressing EYFP or Sig-1R-EYFP were established by transiently transfecting pEYFP-N1 or pEYFP-Sig-1R vectors followed by colony selections with G418 (Geneticin; Invitrogen). Lipofectamine 2000 (Invitrogen) was used for gene transfection. CHO cells were treated with fumonisin B1 (FB1), methyl-β-cyclodextrin (MβC), or cholesterol-conjugated MβC in culture medium without serum. FB1 was dissolved in ethanol and used at 5 μg/ml. MβC was dissolved in phosphate-buffered saline (PBS) and used at 5 mM with 5 μM lovastatin. Cholesterol-conjugated MβC was prepared by rotating 1 ml of MβC solution (100 mM) with N_2-dried cholesterol (4 mg) overnight at room temperature.

DRM Preparation. For the sucrose gradient fractionation of DRMs, CHO cells were cultured in a 10-cm dish at 80 to 90% confluence. CHO cells (2×10^6 cells) were lysed at 4°C in 0.5 ml of TNE-Tx buffer (10 mM Tris at pH 7.4, 150 mM NaCl, 1 mM phenylmethylsulfonyl fluoride, 5 mM EDTA, 48 Kallikrein inactivation units/ml aprotinin, and 0.5% Tx). After being mixed with an equal volume of 80% sucrose, the cell lysate was subjected to sucrose gradient centrifugation at 100,000*g*, and a total of 13 fractions was collected from the top, as described previously (Hayashi and Su, 2003b). The same volume from each fraction was applied to SDS-PAGE.

To prepare the Tx-insoluble pellet enriched with DRMs and the Tx-soluble supernatant by differential centrifugations, cell membranes were incubated in TNE-Tx for 30 min at 4°C. After sonication (10 s, three times), samples were centrifuged at 12,000*g* for 20 min. The supernatant was further centrifuged at 100,000*g* for 1 h in a ^{50}Ti rotor. The pellet and the supernatant were collected as Tx-insoluble (pellet) and Tx-soluble (supernatant) fractions, respectively.

MAM Fractionation. The MAM fraction was prepared as described previously (Rusiñol et al., 1994). In brief, CHO cells were grown on two 15-cm dishes at 90 to 100% confluence. Harvested cells were homogenized by a glass Dounce homogenizer in a homogenization buffer (0.25 M sucrose and 10 mM HEPES/KOH, pH 7.4). The homogenate was centrifuged twice at 500*g* for 5 min to yield the P1 nuclear fraction. The supernatant was spun down at 10,300*g* for 20 min to yield crude mitochondria membranes as a pellet (P2 fraction). The supernatant was centrifuged at 100,000*g* for 1 h in a 50Ti rotor to obtain the P3 microsomal and cytosolic fractions. Crude mitochondrial membranes were suspended in 0.5 ml of isolation medium (250 mM mannitol, 5 mM HEPES/KOH pH 7.4, and 0.5 mM EGTA/KOH), layered on Percoll solution [225 mM mannitol, 25 mM HEPES/KOH, pH 7.4, 1 mM EGTA/KOH, and 30% (v/v) Percoll (GE Healthcare,

Chalfont St. Giles, Buckinghamshire, UK)], and centrifuged at 95,000*g* for 30 min in an SW 55Ti rotor. Purified mitochondrial and MAM fractions were collected and washed twice with an isolation medium by centrifugation.

Immunocytochemistry and Confocal Microscopy. Immunocytochemistry and confocal microscopy were performed as described earlier (Hayashi and Su, 2003b). Primary antibodies were used at 1:100 for anti-Sig-1R or 1:50 for anti-IP3R3. The filipin staining was performed according to a previous report (Hayashi and Su, 2003b).

Lipid Overlay Assay. CHO cells were grown in a 15-cm dish at 90% confluence. Cells were harvested in ice-cold PBS and centrifuged at 2000*g* for 10 min. The cell pellet was suspended in 1 ml of 50 mM Tris, pH 7.4, containing 0.2% CHAPS. The cell lysate was rotated at 4°C for 2 h, followed by a centrifugation at 100,000*g* in a 50Ti rotor for 1 h. The supernatant was filtered by a Millipore 0.22-mm filter unit (Millipore, Billerica, MA). The total protein concentration was measured with a BCA protein assay kit (Thermo Fisher Scientific, Waltham, MA). The lysate was stored at −80°C until use.

Lipids were dissolved in a chloroform/methanol mixture (2:1) and spotted on a Hybond C nitrocellulose membrane (200–10,000 pmol/spot; GE Healthcare). The membrane was air-dried for 1 h at room temperature. The membrane was blocked with TNC buffer (50 mM Tris, pH 7.4, 150 mM NaCl, and 0.2% CHAPS) containing 30% nonfat dry milk and 5% chicken ovalbumin at 4°C for 6 h with gentle shaking. After washings twice with TNC buffer, the membrane was incubated with the CHAPS cell lysate (28–60 μg of protein/cm^2) in TNC containing 150 mM NaCl and 4% BSA at 4°C for 16 h with shaking at 200 rpm. After three washings with TNC containing 3% BSA (each for 10 min), the membrane was incubated with either anti-full-length GFP antibodies (1:1500) or anti-Sig-1R antibodies (1:1000) in TNC with 3% BSA for 3 h at room temperature or 16 h at 4°C. After extensive washings with TNC containing 3% BSA, Sig-1R complexes associated with lipids were detected by horseradish peroxidase-conjugated secondary antibodies, followed by WestFemto chemiluminescence (Thermo Fisher Scientific). Images were captured with Kodak Image Station 440CF (Carestream Health, Rochester, NY).

Lipid Assays. Total lipids were extracted by the Bligh and Dyer method. Free cholesterol in the sample was measured enzymatically by the Free-Cholesterol E kit (Wako Bioproducts, Richmond, VA) or the Cholesterol Assay kit (Sigma-Aldrich). For high-performance thin-layer chromatography (HPTLC; Merck, Darmstadt, Germany), lipid extracts dissolved in the chloroform/methanol mixture (2:1) were spotted on an HPTLC plate followed by resolution with the hexane/ether/acetic acid mixture (16:4:0.2) for cholesterol and neutral lipids and the chloroform/methanol/water mixture (13:5:0.5) for sphingolipids and phospholipids. Lipids were visualized on HPTLC plates using a ferric chloride spray (for cholesterol) or a diphenylamine-aniline spray (for neutral glycosphingolipids). Phospholipids and ceramides were visualized under UV light after spraying 0.2% 8-anilinonaphthalene-1-sulfonate (ANS) in ethanol. The ganglioside-enriched fraction was obtained by applying total lipid extracts to a silicic acid column fractionation followed by Dowex 50 (Na^+ form) and Sep-Pak C18 column chromatography (Waters, Milford, MA). Gangliosides were resolved by HPTLC with chloroform/methanol/0.25% $CaCl_2$ (55:45:10) and visualized by resorcinol or diphenylamine-aniline spray. After separation from other lipids, the ceramides were extracted from an HPTLC plate (Merck) and spotted on a Hybond-C membrane (GE Healthcare). The membrane was blocked with 10% nonfat milk (Bio-Rad Laboratories, Hercules, CA) in PBS followed by incubation with ceramide antibodies (1:200) in the same solution at room temperature for 16 h. After five wash steps with PBS, ceramides on the membrane were visualized as described in the lipid overlay assay.

SDS-PAGE and Silver Staining. Samples were dissolved in a 2× Laemmli sample buffer after protein quantifications (BCA assay kit; Pierce, Rockford, IL). Proteins were separated by SDS-PAGE as described previously (Hayashi and Su, 2003b). Proteins in the acrylamide gel were electrically transblotted to a polyvinylidene difluoride membrane (Bio-Rad Laboratories) in a Towbeen buffer and detected by immunoblotting. Silver stainings were performed according to the company's instruction (Silver Stain Plus; Bio-Rad Laboratories).

Living-Cell Labeling with Fluorescent Ceramides. Fluorescent ceramides (NBD-Cer and BODIPY-Cer TR) were dissolved in the chloroform/methanol mixture (19:1) to a 1 mM concentration. After they were completely dried under N_2, the lipids were dissolved in 200 μl of ethanol. This ethanol solution was injected into 4 ml of Hanks' balanced salt solution supplemented with 10 mM HEPES, pH 7.4, and 12.5 μM BSA under vigorous vortexing. Yielded ceramide-BSA complexes were added at 4°C for 30 min to the culture medium at the final concentration of 1.25 μM followed by washings with ice-cold PBS three times. In the chase experiment, ceramide-labeled cells were returned to the culture incubator with a normal medium. Cells were fixed with 4% paraformaldehyde for 15 min followed by two wash steps with ammonium chloride (5 mM) for 5 min twice and with PBS once.

Results

ER Proteins Associate with DRMs. We examined whether Sig-1Rs and other ER proteins could be found in DRMs extracted from CHO cells. In agreement with previous studies using different types of cells (Hayashi and Su, 2003b, 2004), the sucrose gradient centrifugation of the Tx lysate found that a portion of Sig-1R was indeed present in DRM fractions (Fig. 1A, fractions 4–7). As seen in NG108 cells (Hayashi and Su, 2003b), DRMs associated with Sig-1R showed lower buoyancy in the sucrose gradient (fractions 4–7) than those of Src (fractions 2–5), the protein associated mainly with plasma membrane DRMs. Some ER proteins that are enriched at the MAM, including IP3R3 and BiP, were also present in DRM fractions, although IP3R3 was present at a much lower level (Fig. 1A). Mitofusin-2, the protein tethering MAM to mitochondria (de Brito and Scorrano, 2008), was also detected in DRMs (Fig. 1A). Some ER proteins such as ERp57 were completely excluded from DRMs (Fig. 1A).

Unique Detergent-Solubility Profile of DRMs Associating with Sig-1R. Although Sig-1Rs were consistently detected in DRM fractions in different cell types, the proportion of Sig-1Rs present in DRM fractions is only 10 to 20% of total Sig-1R proteins (Fig. 1A). On the other hand, at least 50% of Src or caveolin was fractionated in DRMs (Fig. 1, A and B). However, it is noteworthy that recent studies demonstrate that DRMs at internal membranes have lower resistance to extraction by the prototypic detergent Tx but exhibit somewhat higher resistance to other types of detergents (Marwali et al., 2003), implying that there are different subclasses of DRMs. Thus, although the marginal level of Sig-1R was present in Tx-insoluble DRMs, the result may not merely imply few Sig-1Rs associated with DRMs. We therefore conducted sucrose gradient centrifugations with different types of detergents. More than 50% of Src and caveolin consistently associated with DRMs in the presence of any type of detergent tested (Fig. 1B). The highest detergent resistance for both proteins was seen with Tx. The detergent resistance was slightly decreased with Brij-35 or Lubrol WX (Fig. 1B). In contrast, detergent resistance of DRMs associated with Sig-1R and IP3R3 dramatically changed depending on the type of detergent used. Among them, DRMs associated with

Sig-1R showed remarkable resistance against extraction with Triton X-114, in which more than 80% of Sig-1Rs were present in DRM fractions (Fig. 1B). Buoyancy of the DRMs was significantly higher in Triton X-114 (fractions 2–4) than that in Tx (Fig. 1B). DRMs associated with IP3R3 exerted significantly higher resistance to extraction by CHAPS, Triton X-114, Brij-35, or Lubrol WX compared with Tx (Fig. 1B). These findings suggest that the high proportion of Sig-1R may be associated with DRMs at the ER, but those are probably much less resistant to extraction by Tx.

The MAM Is the Specialized ER Subdomain Accommodating DRMs. We examined whether the Triton X-114-insoluble DRMs associated with Sig-1Rs is derived from the MAM. As a result, MAM and microsomes were purified from CHO cells, and enrichment of Sig-1R-containing DRMs and DRM-forming lipids was examined in those membranes. In agreement with a previous study (Hayashi and Su, 2007), Sig-1Rs were enriched in the MAM fraction (Fig. 2A). The levels of IP3R3 and certain ER chaperones such as BiP and calreticulin were also the highest in the MAM fraction (Fig. 2A). ER chaperones involved in vesicular transport of proteins were also detected in the cytosolic fraction (Fig. 2A). The ER chaperone ERp57 was more enriched in the microsomal fraction (Fig. 2A). The microsomal protein CYP450R was present exclusively in microsomal and nucleus fractions (Fig. 2A). Mitofusin-2 was present both in mitochondrial and MAM fractions (Fig. 2A). Mitochondria-specific proteins were detected only in the mitochondrial fraction (Fig. 2A). The distribution patterns of these organelle markers thus ver-

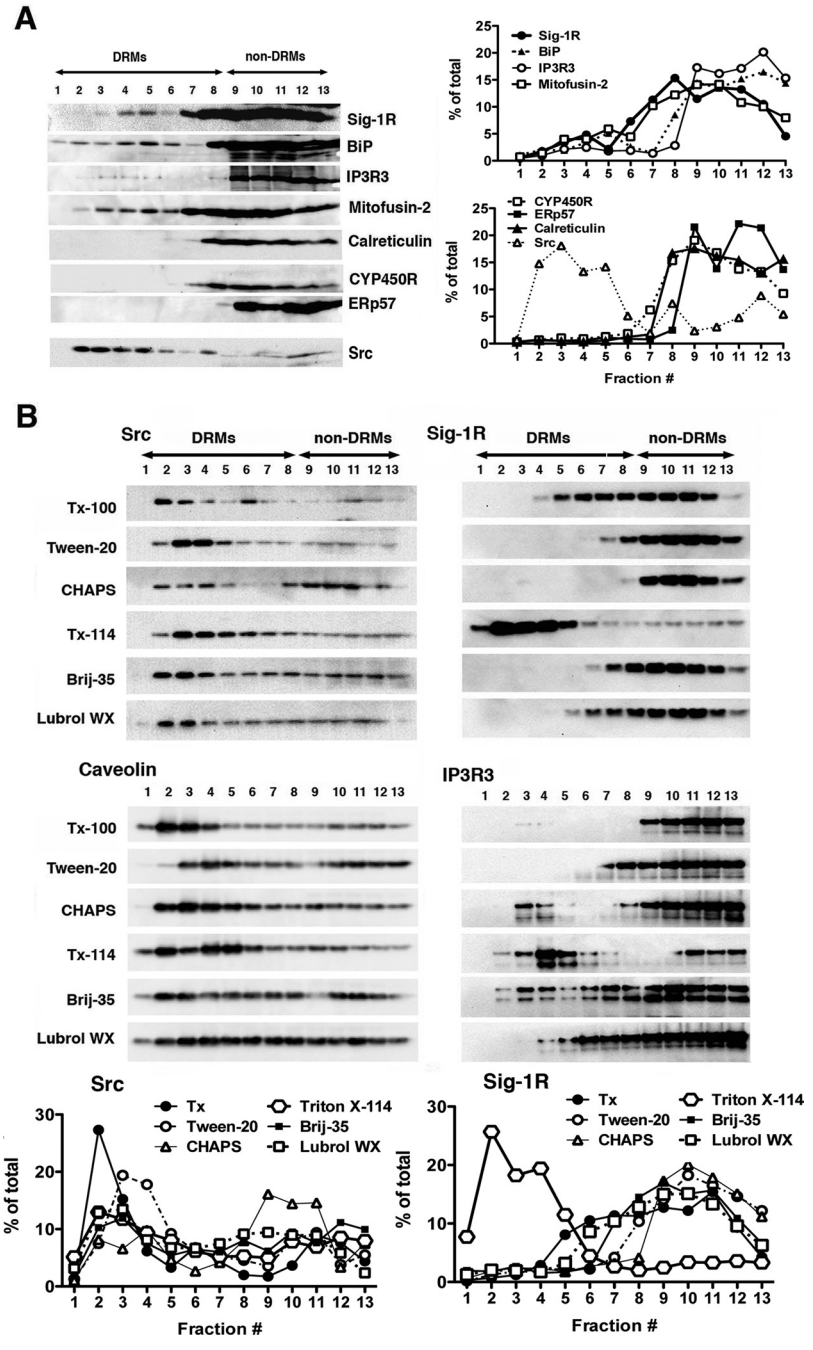

Fig. 1. Detergent-insolubility profile of DRMs associating with Sig-1R. A, ER proteins in DRMs. Tx-cell lysates were fractionated (1–13 from top to bottom) after sucrose gradient centrifugation. Fractions 1 to 8 represent DRMs. Graphs represent fraction distributions of proteins in which the sum of 13 fractions was taken as 100% for each protein (mean of 2–3 experiments). B, solubility of Sig-1R-containing DRMs in different detergents. CHO cells (2×10^6 cells) were solubilized with different detergents (0.5% except for CHAPS at 20 mg/ml), followed by sucrose gradient centrifugation. Proteins enriched at plasma membrane rafts (Src and caveolin) or those at the MAM (Sig-1R and IP3R3) were detected by immunoblotting. Graphs represent fraction distributions of Src and Sig-1R (mean of two experiments).

ified the sufficiently high purity of MAM and microsomal membranes.

When each fraction was solubilized with Tx, a marginal but still detectable level of Sig-1R was present in DRMs from the MAM fraction but not in those from microsomes (Fig. 2B, top). As shown in Fig. 1B, a much higher level of Sig-1Rs was present in DRMs extracted from the MAM with Triton X-114 compared with the extract with Tx (Fig. 2B, bottom). Sig-1Rs were present in DRMs only from the MAM fraction (Fig. 2B), strongly indicating that the Sig-1R-associated DRMs are mostly derived from the MAM. Furthermore, the silver staining showed a much larger amount of proteins present in DRMs derived from the MAM compared with DRMs from microsomes (Fig. 2C), suggesting that the MAM accommodates a higher level of DRMs than the microsome. Indeed, HPTLC revealed that the MAM contains higher levels of DRM-forming lipids, such as cholesterol, ceramides, glucosylceramide (GlcCer), and sphingomyelin, compared with microsomes (Fig. 2D). The higher level of ceramides at the MAM was further confirmed by the lipid overlay assay using anti-ceramide antibodies (Fig. 2D, bottom). Among phospholipids, phosphatidylserine and phosphatidylcholine were present in both membranes at similar levels, but phosphatidylethanolamine was higher in the MAM fraction (Fig. 2D). Lactosylceramide and GM3, the major ganglioside in CHO cells, were not detected in either MAM or microsomes under our HPTLC conditions (data not shown).

The Sig-1R Complex Associates with Specific Sphingolipids. It is well known that DRMs prepared from the plasma membrane mostly consist of cholesterol and complex sphingolipids such as gangliosides. In contrast, DRMs from the MAM seem to be more enriched in simple sphingolipids such as ceramides and GlcCer (Fig. 2D). To examine whether the simple sphingolipids might contribute to the formation of DRMs and the localization of Sig-1R at the MAM, we examined whether Sig-1Rs preferentially associate with those MAM-enriched lipids by using a modified lipid overlay assay. The assay is particularly advantageous in studies using highly hydrophobic molecules as ligands (e.g., lipids), because the assay avoids problematic insolubility/aggregation of ligands and partitioning of ligands into membranes. Because CHAPS (0.2%) solubilization is shown to maintain the ligand-binding property of Sig-1Rs well (McCann and Su, 1991), we used CHAPS cell lysates in the assay. It should be noted, however, that the assay using the CHAPS whole-cell lysate might detect the direct association between lipids and Sig-1R molecules as well as the association between lipids and protein complexes composed of Sig-1R (designated here as the

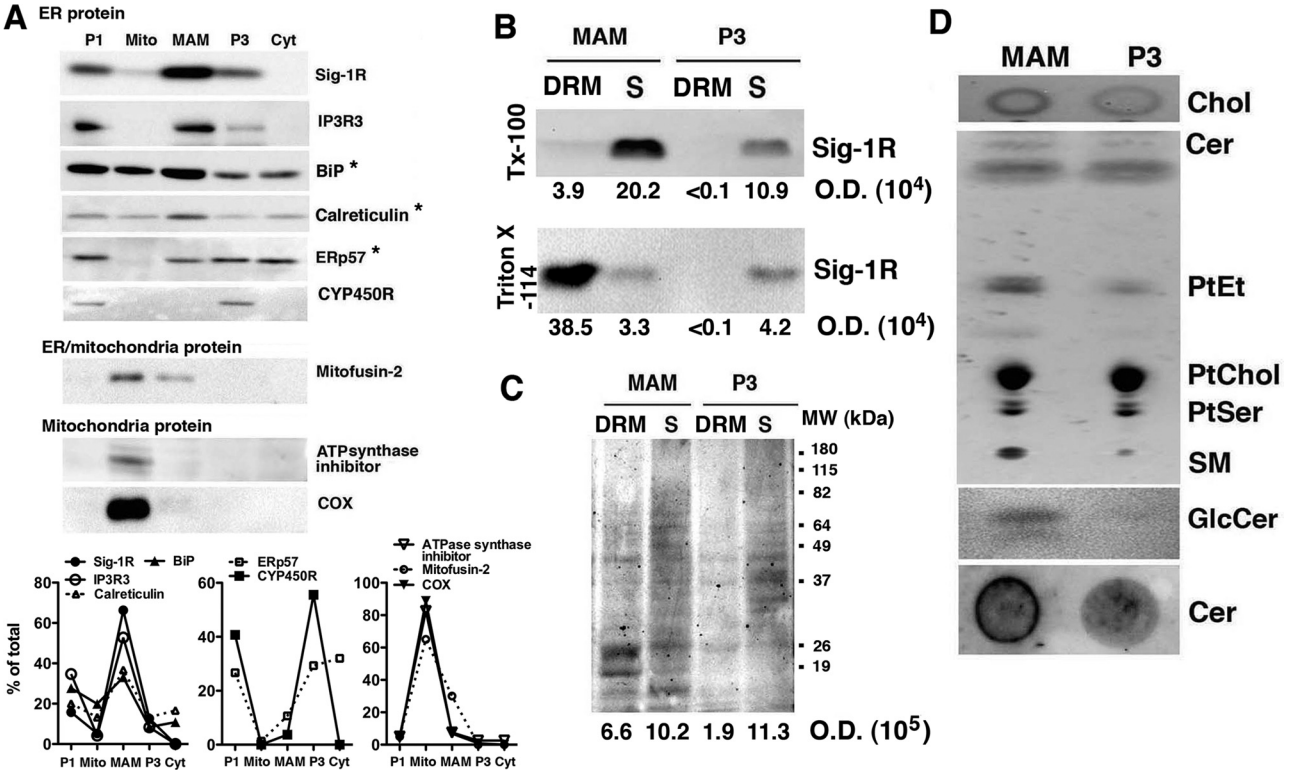

Fig. 2. MAM accommodates DRMs associated with Sig-1R. A, purification of MAM and microsomal fractions from CHO cells. Nuclear (P1), mitochondrial (Mito), MAM, microsomal (P3), and cytosolic (Cyt) fractions were prepared by differential centrifugation combined with a Percoll gradient fractionation. Five micrograms of proteins was applied to SDS-PAGE, followed by immunoblotting. COX, cytochrome *c* oxidase subunit I. Asterisks indicate ER chaperones involved in vesicular transport. Graphs represent fraction distributions of proteins in which the sum of five fractions was taken as 100% for each protein. B, Sig-1R-associated DRMs in the MAM. MAM and microsomes (P3) (25 μg of total proteins in each) were extracted by 0.5% Tx (Tx-100) or Triton X-114 at 4°C. DRMs and detergent-soluble supernatant (S) were prepared by differential centrifugations. The numbers represent the average of optical density (O.D.) measured in each protein band ($n = 3$). C, silver staining for total proteins associated with DRMs in MAM and microsomal fractions. MAM and microsomes (25 μg of total proteins in each) were extracted in 0.5% Tx at 4°C, and DRMs and soluble supernatants (S) were prepared. Proteins were visualized by 13% SDS-PAGE, followed by silver staining. The numbers represent the average of O.D. measured in each lane ($n = 3$). MW, molecular weight of standard proteins. D, lipid contents in MAM and microsomal fractions. Lipids were extracted and analyzed by HPTLC. Cholesterol (Chol) was detected using a ferric chloride spray; GlcCer using a diphenylamine-aniline spray. Lipids in the second panel were visualized under UV light after an ANS spray. In the lipid overlay assay for ceramides (Cer, bottom), ceramides extracted from HPTLC plates were immobilized on a nitrocellulose membrane followed by immunoblotting with anti-ceramide antibodies. SM, sphingomyelin.

"Sig-1R complex"). The commercially available SphingoStrips Array membrane (200 pmol/spot; Invitrogen) demonstrated that Sig-1R-EYFP complexes from the CHAPS lysate of Sig-1R-EYFP-overexpressing CHO cells specifically associate with ceramide and sulfatide of 15 different lipids immobilized on the array membrane (Fig. 3A). No association of Sig-1R-EYFP complexes with sphingosine, sphingomyelin, or sphingosine-1-phosphate was observed under these conditions (Fig. 3A); however, the association between Sig-1R complexes and sphingosine was consistently detected when the lipid on the array was increased to 1 nmol/spot. Solubilized EYFP complexes obtained from CHO cells stably overexpressing EYFP did not associate with any lipids on the array (Fig. 3A).

To further examine lipids interacting with Sig-1R complexes, we prepared a nitrocellulose array membrane with 30 different lipids immobilized (200 pmol/spot). The assay found that Sig-1R-EYFP complexes associated preferentially with sphingolipids with few or no sugar moieties but not with gangliosides [association potency: lactosylceramide > galactosylceramide > glucosylceramide > sulfatide > hydroxy or nonhydroxy ceramide (from bovine brains) ⋙ gangliosides] (Fig. 3B). The two oligodendrocyte-specific glycosphingolipids, galactosylceramide and sulfatide, were both capable of associating with Sig-1R-EYFP complexes (Fig. 3B). It is interesting that among sterols tested under this condition, only lathosterol showed a detectable yet low association with Sig-1R-EYFP complexes (Fig. 3B). This result is in agreement with the fact that the Sig-1R shares 66% similarity with a yeast C8–C7 sterol isomerase catalyzing the conversion of zymosterol to lathosterol (Hanner et al., 1996). Endogenous Sig-1R complexes also showed a similar profile in the lipid binding, but with lower signals, thus prohibiting the detection of some interactions (Fig. 3C). This seemed to be mainly due to the lower protein level of endogenous Sig-1R complexes in the lysate. Increasing the total protein level in the lysate (from 28 to 60 μg of protein lysate/cm^2 of membrane),

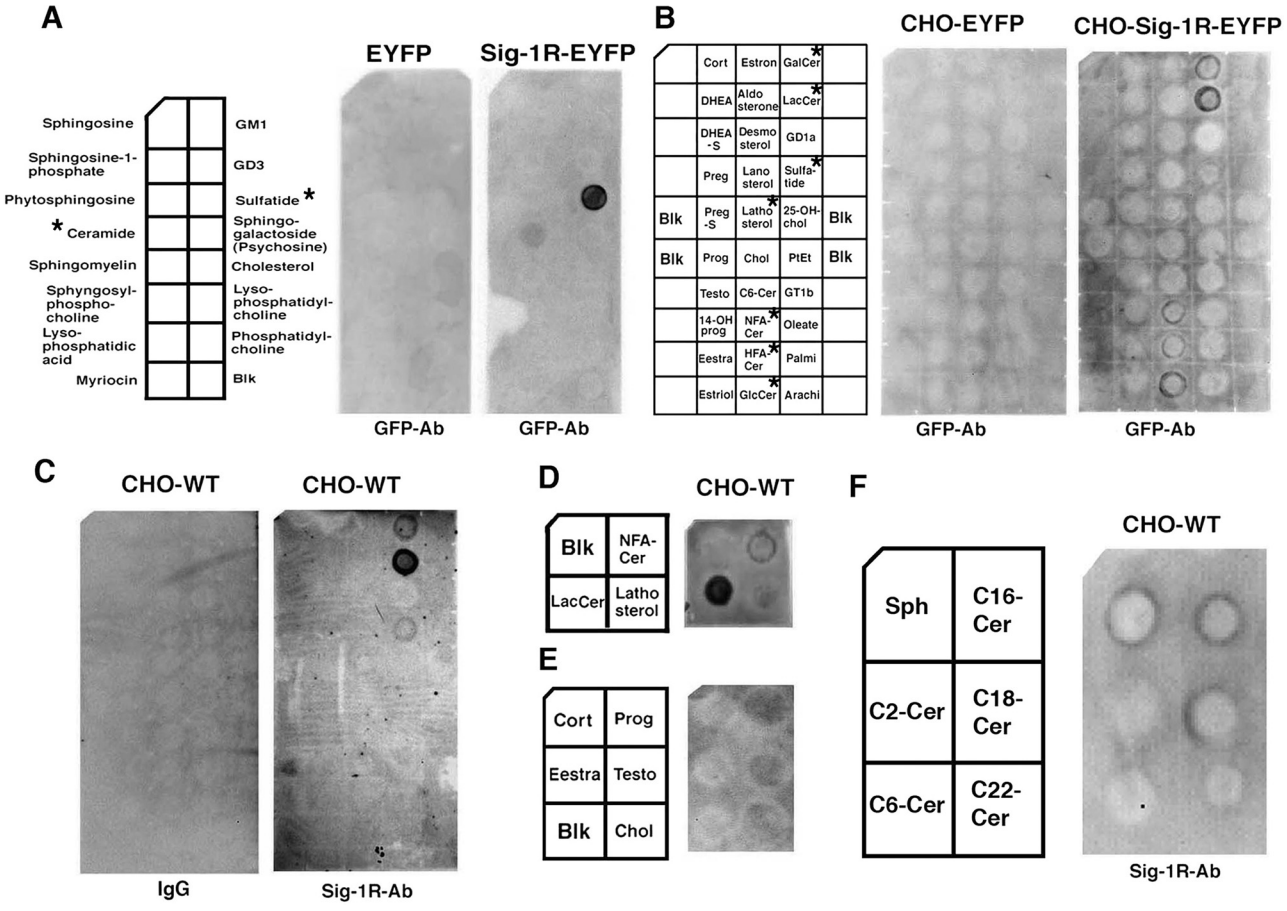

Fig. 3. Association of simple sphingolipids with solubilized Sig-1R complexes. A, lipid overlay assay using the SphingoStrips Array membrane (200 pmol/spot). CHO cells stably expressing either EYFP or Sig-1R-EYFP were solubilized with 0.2% CHAPS. CHAPS cell lysates (28 μg of total proteins/cm^2) were incubated with the array membrane followed by immunodetections with anti-GFP antibodies. Blk, blank. Asterisks indicate lipids identified as being associated with Sig-1R-EYFP. B, association of Sig-1R-EYFP complexes with simple sphingolipids. CHO cell lysates were incubated with Hybond-C Extra nitrocellulose membranes, 30 different lipids (200 pmol/spot) were immobilized. Cort, corticosterone; DHEA (-S), dehydroepiandrosterone (-sulfate); Preg (-S), pregnenolone (-sulfate); Prog, progesterone; Testo, testosterone; Eestra, estradiol; Chol, cholesterol; Cer, ceramide; NFA-Cer, Cer with nonhydroxy fatty acid; HFA, hydroxy fatty acid; Palmi, palmitate; Arachi, arachidonate. Asterisks indicate lipids identified as being associated with Sig-1R-EYFP. C, association of endogenous Sig-1R complexes with lipids. Wild-type CHO cells were solubilized with 0.2% CHAPS and the lysates were incubated with the nitrocellulose membranes. The left membrane was developed with normal rabbit IgG and the right with specific anti-Sig-1R antibodies. D, association of endogenous Sig-1R complexes with ceramides, lactosylceramides (LacCer) and lathosterol. Note that each spot contains 400 pmol of lipid. The membrane was incubated with a cell lysate from wild-type CHO cells at a total protein concentration of 60 μg/cm^2. Sig-1Rs associated with the lipids were detected by anti-Sig-1R antibodies. E, the association of endogenous Sig-1R complexes with sterols. Each spot contains 10 nmol lipid. The membrane was incubated with a cell lysate from wild-type CHO cells at a total protein concentration of 60 μg/cm^2. F, association of endogenous Sig-1R complexes with ceramides and sphingosine. D-*erythro*-sphingosine (Sph), C2-Cer, and C6-Cer are at 1 nmol/spot. Other ceramides are at 400 pmol/spot. The protein concentration of the CHAPS lysate is 60 μg/cm^2 of membrane.

accompanied by increased lipids on the membrane (400 ≥ pmol/spot), ensured the reproducible detection of endogenous Sig-1R complexes associated with ceramides or lathosterol (Fig. 3D).

It has been demonstrated that Sig-1Rs associate with certain steroids and cholesterol (Su et al., 1988; Pal et al., 2007; Palmer et al., 2007). Indeed, the assay detected the association of Sig-1Rs with some sterols (lathosterol ≫ progesterone ≥ testosterone ⋙ cholesterol), but much higher amounts of lipids (10 nmol/spot) were necessary, except for lathosterol, to obtain reliable signals (Fig. 3E).

D-*erythro*-Sphingosine associated with Sig-1R complexes (Fig. 3F). However, in contrast to the previous report (Ramachandran et al., 2009), the interaction between the Sig-1R complex and ceramide was consistently detected. Ceramides possessing a long fatty acid acyl chain (i.e., C16–18), which is naturally present, associated better with Sig-1R complexes, whereas synthetic ceramides with short acyl chains (e.g., C6, C2) failed to associate with Sig-1R-EYFP or Sig-1R complexes (Fig. 3, B and F). The estimated order of potencies of ceramides/sphingosine in associating with Sig-1R complexes was C18-ceramide = C16-ceramide > D-*erythro*-sphingosine > C22-ceramide ⋙ C6-, C2-ceramides. The structures of these lipids are provided in the supplemental figure.

Because the MAM is shown to possess high ceramide biosynthesis activity (Bionda et al., 2004), we focused particularly in the following studies on ceramides to determine whether the lipid may play a role in the localization of Sig-1R to the MAM.

MAM Is Highly Capable of Accumulating Ceramides. An early study demonstrates that exogenously applied fluorescent NBD-Cer distributes heterogeneously in living cells. NBD-Cer accumulate initially at the plasma membrane and ER and then at mitochondria in living cells when they are incubated at 2°C, a temperature at which energy-dependent vesicle transport of lipids is shut down (Lipsky and Pagano, 1983). This finding clearly illustrates that the intermembrane diffusion of ceramides from the ER to the mitochondrial membranes is restricted at the ER-mitochondria junction. Thus, the MAM might be highly capable of accumulating ceramides to serve as the checkpoint regulating the diffusion of ceramides from the ER to the mitochondria. To examine whether the MAM accumulates ceramides, CHO cells were incubated with NBD-Cer at 4°C, and the cellular distribution was monitored by confocal mi-

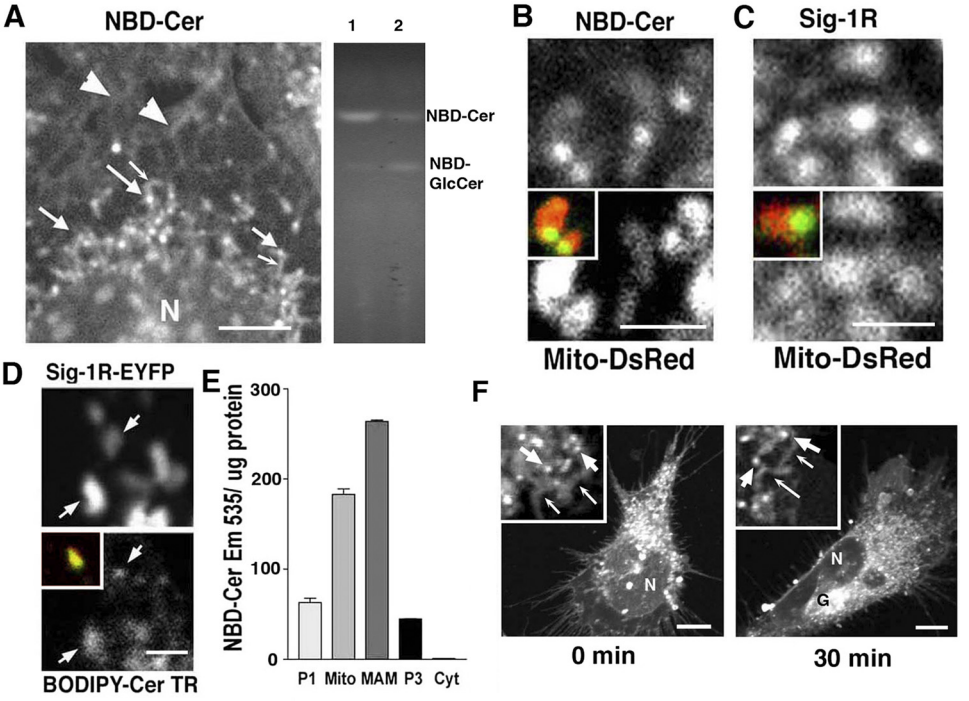

Fig. 4. MAM accumulates ceramides. A, accumulation of NBD-Cer at subcellular membranes. CHO cells were incubated with NBD-ceramide (1.25 μM) at 4°C for 30 min. Confocal microscope (left). Arrowhead, ER cisternae; small arrow, mitochondria with a spaghetti-like shape; large arrow, juxta-mitochondria structures accumulating NBD-Cer; N, nucleus. Bar, 10 μm. HPTLC (right), where lipid extracts from NBD-Cer-labeled CHO cells were visualized under UV. 1, the lipid extract from CHO cells incubated with NBD-Cer at 4°C for 30 min; 2, the lipid extract from CHO cells incubated with NBD-Cer at 4°C for 30 min, followed by washings and incubation at 37°C for 30 min. Note the few conversions of NBD-Cer to NBD-GlcCer in lane 1. B, accumulation of NBD-Cer at intracellular domains apposing mitochondria. NBD-Cer (top) and mitochondria expressing Mito-DsRed (bottom) were visualized in the same cell. The two panels were superimposed in the inset (NBD-Cer in green, MitoDsRed in red). Bar, 2.5 μm. C, MAM-specific distribution of Sig-1R (top; in green inset). Shown at the bottom is mitochondria in the same sample. Bar, 2.5 μm. Inset, two panels superimposed. D, colocalization between Sig-1R-EYFP and fluorescent ceramides. CHO cells expressing Sig-1R-EYFP (top) were labeled with fluorescence ceramide BODIPY-Cer TR (1.25 μM; bottom) at 4°C for 30 min. Inset, two panels are superimposed (Sig-1R-EYFP in green, BODIPY-Cer TR in red). Bar, 2.5 μm. Inset, colocalization is represented by yellow. The same results were obtained from four independent samples (>5 fields/sample). E, MAM accumulates NBD-Cer. CHO cells labeled with NBD-Cer at 4°C for 30 min were subjected to membrane fractionations. The level of NBD-Cer in each fraction was measured by a fluorescence microplate reader. Fluorescence intensities were normalized to protein concentrations in each sample. F, retention of NBD-Cer at MAM. CHO cells were labeled with NBD-ceramides at 4°C for 30 min (left image). After washings, cells were incubated in normal medium at 37°C for 30 min (right image). Thin arrows, mitochondria; thick arrows, MAM; N, nucleus; G, Golgi apparatus; Bar, 10 μm.

croscopy. As expected, a striking accumulation of NBD-Cer was observed at MAM-like small structures (Fig. 4A, large arrows) juxtaposed to mitochondria that bear the typical spaghetti-like structure (Fig. 4A, small arrows). NBD-Cer also accumulated at the cisternae of the ER (Fig. 4A, arrowheads) and the mitochondria, but at much lower levels. The observed NBD signals in living CHO cells seem to represent mostly the distribution of NBD-Cer, but not that of those metabolites, because few NBD-Cer were metabolized to GlcCer in the living cells under 4°C (Fig. 4A, lane 1). The structures accumulating NBD-Cer clearly apposed mitochondria that were visualized by expressing Mito-DsRed (Fig. 4B), and the staining pattern was identical with that of Sig-1R immunostaining (Fig. 4C). The other fluorescent ceramide (BODIPY-Cer TR) accumulated similarly at the MAM-like structures that colocalized with Sig-1R-EYFP (Fig. 4D). Membrane fractionation confirmed that the level of NBD-Cer is the highest in the MAM fraction (Fig. 4E).

To examine whether the accumulation of ceramides at the MAM is adversely affected by the low-temperature incubation, under which vesicular transports of lipids from ER to Golgi are stalled, cells labeled with NBD-Cer were returned to the normal culture condition at 37°C. Under these conditions, NBD-Cer accumulated at the Golgi apparatus but decreased at the ER (Fig. 4F), indicating that the energy-dependent transport of ceramides from ER to Golgi was now resumed. Under these conditions, a portion of NBD-Cer was converted to GlcCer (Fig. 4A, lane 2 of TLC); the step is known to be mainly catalyzed at the Golgi. It is important to note that even under these conditions, the MAM still accommodated a significant level of NBD-Cer, suggesting that the MAM may possess the innate ability to accumulate ceramides at the locus.

Although the distribution of NBD-Cer may not necessarily represent precise cellular dynamics of endogenous ceramides, the finding that MAM can attract NBD-Cer and accommodate the high level of endogenous ceramides (Fig. 2D) suggests that Sig-1R complexes that possess affinities for ceramides might be preferentially recruited to the ER subdomain.

Sig-1Rs Require Ceramides for Their Partitioning into DRMs. To examine the importance of ceramides in localization of Sig-1Rs at the MAM, we used pharmacological approaches that enable the manipulation of lipid contents and DRM integration at the ER membranes. MβC is a well known compound that depletes free cholesterol in biological membranes, thus disrupting DRMs (Simons and Toomre, 2000). Because water-soluble MβC does not readily penetrate plasma membranes, we assumed that MβC might extract cholesterol initially at the cell surface. On the other hand, the long exposure to MβC is known to cause a nearly complete depletion of cholesterol in the whole cell (Naslavsky et al., 1999). As a result, CHO cells were treated with MβC for different periods of time to preferentially destroy DRMs either at the cell surface or in the entire cell. Incubation with MβC for 15 min depleted 30% of total cholesterol in CHO cells, whereas incubation for 60 min depleted approximately 80% of total cholesterol (Fig. 5A). Filipin staining confirmed that a short exposure to MβC reduced cholesterol mainly on the cell surface, but a longer exposure decreased cholesterol in the entire cell (Fig. 5B). Next, we examined the effect of MβC on partitioning of proteins to DRMs. The treatment with MβC for 15 min significantly decreased Src associated with DRM but not Sig-1R (Fig. 5E), suggesting that Sig-1R-residing DRMs are intracellularly localized. On the other hand, a long exposure to MβC (for 60 min) significantly

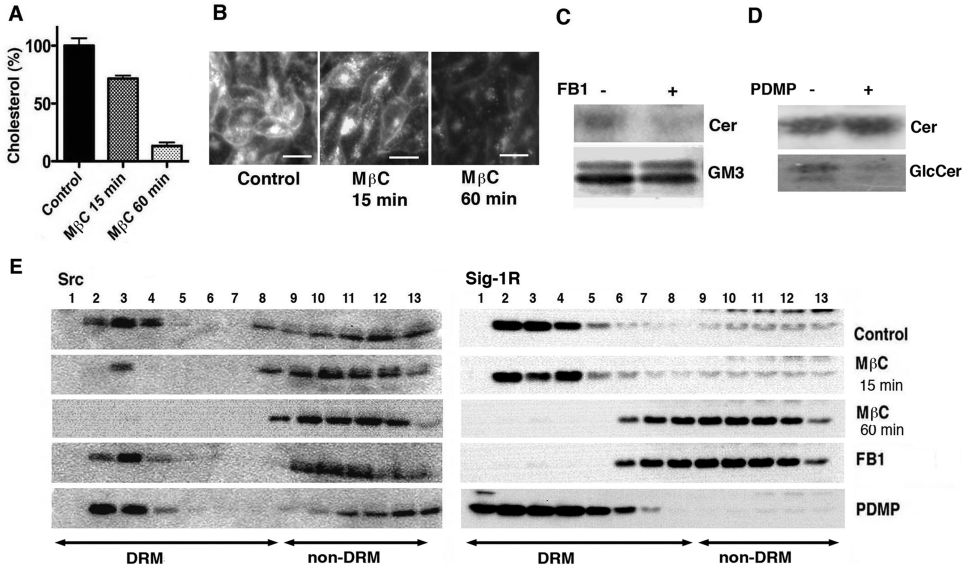

Fig. 5. Cholesterol and ceramide-dependent partitioning of Sig-1R into DRMs. A, time-dependent depletion of free cholesterol caused by MβC. CHO cells in a serum-free medium were incubated with 5 mM MβC. Lipids were extracted, and free cholesterol was measured enzymatically. The graph represents the mean ± S.E.M. from five results. B, time-dependent depletion of free cholesterol caused by MβC. CHO cells treated with MβC for 15 or 60 min were fixed and stained with filipin. Bar, 50 μm. Results from five independent experiments are shown. C, depletion of ceramides at the MAM caused by FB1 (5 μg/ml, 4 h). Ceramides were extracted from MAM fractions. GM3 gangliosides were extracted from whole cells. Representative results from three independent HPTLC are shown. Lipids were visualized by ANS (top) and diphenylamine-aniline (bottom) sprays, respectively. D, PDMP (25 μg/ml, 4 h) decreases GlcCer but accumulates ceramides. Ceramides and GlcCer were extracted from whole cells. Representative results from three independent HPTLCs are shown. Lipids were visualized by ANS (top) and diphenylamine-aniline (bottom) sprays, respectively. E, effects of depletion of cholesterol or ceramide on partitioning of Src and Sig-1R to DRMs. Src-containing DRMs were extracted by 0.5% Tx whereas Sig-1R-containing DRMs were extracted by 0.5% Triton X-114. CHO cells were treated with MβC, FB1, or PDMP under the same conditions in B to D.

decreased Sig-1R in DRMs (Fig. 5E), indicating that Sig-1R-residing microdomains also require cholesterol for stabilization/formation.

FB1, which blocks the conversion of sphinganine to dihydroceramide, is a potent inhibitor of the ceramide biosynthesis at the ER (Naslavsky et al., 1999). Although FB1 rapidly inhibits the synthesis of ceramides at the ER, FB1 requires prolonged incubation (e.g., 24–72 h) to deplete gangliosides or sphingomyelin in the cell because of their slow turnover rates and/or the alternative synthesis pathways independent of de novo synthesis of ceramides (Naslavsky et al., 1999). Because the MAM serves as the locus for ceramide biosynthesis (Bionda et al., 2004) and it is assumed that the major pool of ER ceramides relies on activity of the de novo synthesis at the ER (Sprong et al., 2001), we expected that FB1 might efficiently and rapidly decrease the focal concentration of ceramides at the MAM. In fact, FB1, even with its treatment for 4 h, significantly reduced ceramides at the MAM without largely affecting total levels of ganglioside GM3 in CHO cells (Fig. 5C). As shown previously (Naslavsky et al., 1999), prolonged incubation with FB1 (24 h) significantly decreased GM3 in CHO cells (data not shown). Next, we examined whether the depletion of ceramides caused by FB1 might affect the association of Sig-1R with DRMs. As shown in Fig. 5E, treatment with FB1 for 4 h significantly decreased Sig-1R associated with DRMs. However, little effect on Src association with plasma membrane DRMs was observed, suggesting that ceramides are important molecules for partitioning of Sig-1R to DRMs.

FB1 may also reduce metabolites such as GlcCer, which might be components of DRM at the MAM, immediately downstream of the ceramide synthesis. GlcCer is synthesized by a GlcCer synthase at the cytoplasmic surface of the Golgi apparatus (Sprong et al., 2001). The GlcCer synthesis depends largely on ceramides supplied by the de novo synthesis at the ER (Sprong et al., 2001). Thus, inhibition of the GlcCer synthesis by (±)-*threo*-1-phenyl-2-decanoyl-amino-3-morpholino-1-propanol hydrochloride (PDMP) decreased GlcCer, whereas it concomitantly accumulated ceramides in the cell (Fig. 5D). We next examined whether PDMP affects the association of Sig-1R with DRMs. PDMP (4 h) unexpectedly increased Sig-1R association with DRMs (Fig. 5E), indicating that ceramides, but not GlcCer, seem to serve as a positive regulator of Sig-1R for their partitioning into DRMs.

DRMs Anchor Sig-1R at the ER-Mitochondria Junction. To assess the importance of DRMs in MAM-specific distribution of Sig-1R, we tested whether disruption of DRMs may affect the cellular localization of Sig-1R. Treatment with MβC (60 min) or FB1 (4 h) caused a dramatic redistribution of Sig-1R-EYFP from MAM to ER cisternae (Fig. 6A), resulting in a significant reduction in Sig-1R-EYFP colocalization with Mito-DsRed (Fig. 6B). MβC presaturated with cholesterol (MβC-Chol), which provides free cholesterol to the cell, failed to promote the translocation of Sig-1R-EYFP (Fig. 6A). MβC-Chol, however, did cause swelling of the mitochondria (Fig. 6A; round mitochondria shown in red), as reported previously (Colell et al., 2003). This redistribution seemed to be due to the translocation of Sig-1R-EYFP at ER membranes but not due to structural disorganization of ER membranes caused by MβC or FB1, because the treatments did not significantly alter the overall structure of ER membranes or the spatial interaction between ER membranes and mitochondria at least under observations with confocal microscopy (Fig. 6, C and D, middle). The confocal analysis revealed that these treatments do not alter colocalization of fluorescence signals derived from Mito-GFP and KDEL-DsRed (Fig. 6C). The treatment with MβC or FB1 also caused a similar redistribution of IP3R3 originally present at the MAM (Fig. 6D). Thus, cholesterol and ceramides are important membrane components at the ER for anchoring Sig-1R at the MAM.

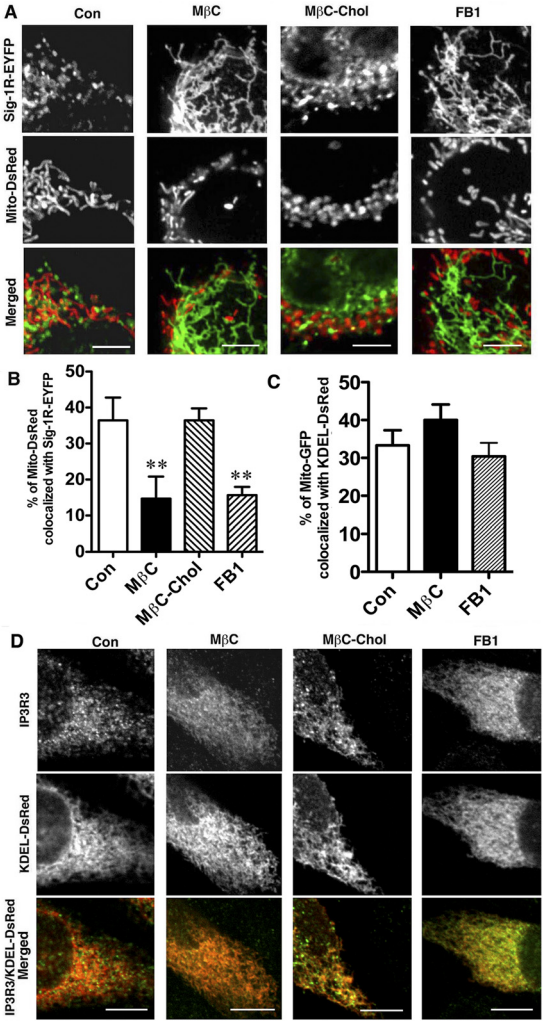

Fig. 6. Relocation of MAM proteins caused by depletion of cholesterol or ceramides A, relocation of Sig-1R-EYFP from MAM to ER cisternae. CHO cells expressing Sig-1R-EYFP (in green) and Mito-DsRed (mitochondria in red) were treated with MβC (5 mM for 60 min), MβC-chol (5 mM for 60 min), or FB1 (5 μg/ml for 4 h). Cells were fixed and observed under a confocal microscope. Bar, 10 μm. B, quantitative analyses for Sig-1R-EYFP in the vicinity of mitochondrial membranes. The percentage of Mito-DsRed colocalizing with Sig-1R-EYFP was analyzed by the PerkinElmer UltraView system (n = 6–7, mean ± S.E.M.) (PerkinElmer Life and Analytical Sciences, Waltham, MA). **, $p < 0.01$ compared with control by one-way analysis of variance followed by Tukey post hoc test. C, no effect of MβC (5 mM for 60 min) or FB1 (5 μg/ml for 4 h) on the association between ER and mitochondrial membranes. Colocalization between KDEL-DsRed (ER membrane) and GFP-Mito (mitochondria membrane) was assessed as described in B. D, relocation of IP3R3 from MAM to ER cisternae. Drugs were applied to CHO cells under the same conditions as in A. IP3R3 (in green) were immunostained with anti-IP3R3 antibodies in cells expressing KDEL-DsRed (in red) for ER. Bar, 10 μm.

Discussion

Our findings indicate that ER-residing DRMs play an important role in the targeting of Sig-1Rs to the ER-mitochondria junction. A unique characteristic of the MAM shown in this study is the enrichment of DRM-forming lipids at the locus (e.g., cholesterol, ceramide), which are normally low at ER membranes (Sprong et al., 2001). It is interesting that Sig-1R-containing DRMs formed at the MAM showed much higher resistance to Triton X-114 than to Tx. This characteristic is different from that of DRMs derived from plasma membranes. On the other hand, σ-2 receptors are shown to associate with DRMs that share similar characteristics with those of plasma membrane DRMs (e.g., high resistance to extraction by Tx) (Gebreselassie and Bowen, 2004). Therefore, it is uncertain whether the Sig-1R-containing DRMs may serve as a subtype of so-called lipid rafts or whether they represent novel lipid microdomains biophysically dissimilar to lipid rafts.

The MAM plays a pivotal role at the ER by regulating ER-mitochondria communications (Hajnóczky et al., 2006; Rizzuto and Pozzan, 2006). Ca^{2+} influxed from the MAM to the mitochondria activates the tricarboxylic acid cycle, whereas overloading of Ca^{2+} in mitochondria causes apoptosis (Hajnóczky et al., 2006; Rizzuto and Pozzan, 2006). Several important metabolites are transported between the ER and the mitochondria via the MAM, including phospholipids, cholesterol, and ATP (Hayashi et al., 2009). To properly operate the interorganelle transport and signal transduction, the MAM is equipped with particular sets of proteins, such as Ca^{2+}-sensitive molecular chaperones, IP3 receptors, Ca^{2+}/ATPase, phosphatidylserine synthase, ubiquitin ligase, and mitofusin-2 (de Brito and Scorrano, 2008; Hayashi et al., 2009). Thus, defining the molecular mechanisms underlying the targeting of specific proteins to the MAM is of utmost importance for understanding of the fundamental functions of the cell. Here we demonstrated one potential mechanism by which the MAM can accommodate specific proteins at the locus. To be exact, the MAM uses detergent-resistant lipid microdomains to recruit proteins to the ER-mitochondria junction. It is worth noting that DRMs also play an important role in recruiting specific proteins at the junction between the plasma membrane and ER (Pani et al., 2008). One study demonstrates that caveolae-type DRMs determine the targeting of STIM1 clusters to ER-plasma membrane junctions after depletion of ER Ca^{2+} (Pani et al., 2008). Therefore, although the sphingolipid components of DRMs vary depending on the location, they might be used more commonly to recruit specific proteins to focal contacts of organelles.

It has been shown that Sig-1Rs bind sterols (Su et al., 1988; Palmer et al., 2007). Furthermore, a recent study finds that D-*erythro*-sphingosine and sphinganine, but not sphingosine-1 phosphate, bind with Sig-1R in a manner competitive to the prototypic Sig-1R agonist (+)pentazocine (Ramachandran et al., 2009). In this study, a lipid overlay assay demonstrated that the CHAPS-solubilized Sig-1R complex possesses affinities for ceramides and mono/diglycosylated ceramides but not for gangliosides and sphingomyelin. In agreement with the study done by Ramachandran et al., (2009), the lipid overlay assay demonstrated that the solubilized Sig-1R complex preferentially binds to sphingosine. However, a previous study reports no association between Sig-1R and ceramides using in vitro binding assays (Ramachandran et al., 2009). Potential explanations for this discrepancy are 1) the association of ceramides with the Sig-1R complex might require the integrated oligomeric protein complex containing Sig-1R, thus the association may not be achieved with purified Sig-1R; 2) ceramides could be interacting with regions of Sig-1R that are not involved in ligand binding; 3) ceramides bearing a long acyl chain (>C16) are highly insoluble and easily aggregated in aqueous conditions if amphiphilic carrier molecules such as albumin are absent (Siskind et al., 2006), thus aggregated ceramides might lose their affinity for Sig-1R in the binding assay; or 4) the length of the acyl chain of the ceramide used by Ramachandran et al., (2009) might be different from the one described here (the length is critical for the association with Sig-1R complexes; Fig. 3F). In contrast to sphingosine possessing the ionizable nitrogen atom, ceramides possess the nitrogen atom as an amide, thus not providing a possible interaction of the nitrogen head with its unshared electrons to interact directly with the Sig-1R-binding site. Therefore, the pharmacophore of these lipids used in association with Sig-1R might not be completely identical. On the other hand, it is also possible that the ceramides are regulating the distribution of the Sig-1R-containing microdomains by interacting with accessory proteins in the microdomain and not selectively with the Sig-1R.

Although sphingosine possesses an affinity for Sig-1R in the nanomolar range, the lipid is not likely to be the constituent of Sig-1R-associated DRMs at the MAM. As a metabolic intermediate of the rapid ceramide biosynthesis, sphingosine is kept at a considerably low level in the cell, especially under unstressed conditions (Spiegel and Milstien, 2003). Sphingosine is physicochemically categorized as a class III lipid (i.e., a swelling amphiphile that possesses strong polar groups of the aminoalcohol head) that renders the molecule soluble in water at low concentrations (Shen et al., 2001). Furthermore, a previous study showed that sphingosine (at higher concentrations) is taken up by the membrane via a passive diffusion mechanism independent of lipid raft integrity (Garmy et al., 2005). Because sphingosine is a water-soluble lipid that quickly changes its concentration under cellular stress (e.g., via its phosphorylation) (Spiegel and Milstien, 2003), the lipid may rather serve as an important Sig-1R ligand that is called upon under pathological conditions. On the other hand, ceramides that are integrated in bilayer membranes might serve as an anchor tethering Sig-1R complexes to the ER-mitochondria junction.

Our data suggested that ceramide is a sphingolipid component constituting Sig-1R-containing DRMs at the MAM. PDMP that decreases GlcCer while concomitantly accumulating ceramides at the ER (Naslavsky et al., 1999) did increase partitioning of Sig-1R to DRMs. However, one unsolved question arising from this finding is why GlcCer, which is enriched at the MAM (Fig. 2D) and possesses a strong affinity for Sig-1R complexes in vitro (Fig. 3B), failed to substitute for ceramides in partitioning Sig-1R to DRMs. To explain this, we propose the asymmetric membrane model of the MAM in which ceramides and GlcCer may be distributed at the inner and outer leaflets of the MAM, respectively. Although ceramides are synthesized at the cytoplasmic surface of ER membranes (Sprong et al., 2001), the rate of their spontaneous transbilayer movement is relatively rapid and

less restricted because of the small polar head (Sprong et al., 2001). Furthermore, ceramides remaining at the cytoplasmic leaflet might be readily transported to the mitochondria via the intermembrane transport or to the Golgi via the ceramide transport protein (Sprong et al., 2001). Therefore, it is possible to speculate that ceramides and their containing DRMs might be confined to the lumenal leaflet of the MAM. However, GlcCer is shown to function on the cytosolic surface of membranes to regulate the budding of transport vesicles (van Meer et al., 2003). Furthermore, it is suggested that Sig-1R form a ligand-binding site at the lumenal surface of the ER membrane (Pal et al., 2007; Hayashi and Su, 2008), the region assumed to interact with prototypic Sig-1R ligands as well as with sphingosine and sterols (Palmer et al., 2007; Ramachandran et al., 2009). Therefore, our asymmetry model of the MAM implies that GlcCer at the cytoplasmic leaflet of the MAM may have less probability of associating with the lipid-binding domain of Sig-1R in in vivo systems. In contrast, galactosylceramide that is synthesized at the ER lumen of oligodendrocytes may be able to associate with Sig-1R, as reported previously (Hayashi and Su, 2004).

In conclusion, our findings demonstrate that the MAM uses ceramide-rich lipid microdomains to anchor Sig-1R at the locus. The lipid microdomains at the organelle junction may therefore play crucial roles in positioning Sig-1R for cellular survival and mitochondrial bioenergetics. The most interesting question for future studies is whether and how Sig-1R agonists or antagonists alter the association of Sig-1R complexes with DRMs, particularly with ceramides therein. It is unclear whether Sig-1R ligands could promote the dissociation of Sig-1R from ceramides that are basically buried in membrane bilayers. On the other hand, it is known that cellular stress per se affects the metabolisms of ceramides (e.g., the breakdown of sphingomyelin to ceramide or ceramide to sphingosine) and membrane integrations, including DRMs (Sprong et al., 2001; Spiegel and Milstien, 2003). Therefore, another important question that awaits future study is whether stress-induced alterations of membrane lipids and their integration at DRMs might represent the intrinsic mechanism by which translocation of Sig-1R is regulated in the cell. Because the dynamic redistribution is a key element for Sig-1R chaperones to determine their client proteins localized at either plasma membranes or the ER, elucidating molecular mechanisms by which the cell switches the action site of Sig-1R may help to further understand the function of Sig-1R and to develop a new class of therapeutic drugs.

Acknowledgments

We thank Dr. Tsung-Ping Su, Cellular Pathobiology Section, National Institute on Drug Abuse, National Institutes of Health, for fruitful discussion throughout the project and comments on the manuscript. We also thank Eri Hayashi and Abasha Lewis, Cellular Pathobiology Section, National Institute on Drug Abuse, National Institutes of Health, for technical assistance and manuscript editing, respectively. We also thank the National Institutes of Health Fellows Editorial Board for assistance in editing the manuscript and providing important editorial comments.

References

Aydar E, Palmer CP, Klyachko VA, and Jackson MB (2002) The sigma receptor as a ligand-regulated auxiliary potassium channel subunit. *Neuron* **34:**399–410.

Bionda C, Portoukalian J, Schmitt D, Rodriguez-Lafrasse C, and Ardail D (2004) Subcellular compartmentalization of ceramide metabolism: MAM (mitochondria-associated membrane) and/or mitochondria? *Biochem J* **382:**527–533.

Bowen WD (2000) Sigma receptors: recent advances and new clinical potentials. *Pharm Acta Helv* **74:**211–218.

Colell A, García-Ruiz C, Lluis JM, Coll O, Mari M, and Fernández-Checa JC (2003) Cholesterol impairs the adenine nucleotide translocator-mediated mitochondrial permeability transition through altered membrane fluidity. *J Biol Chem* **278:**33928–33935.

de Brito OM and Scorrano L (2008) Mitofusin 2 tethers endoplasmic reticulum to mitochondria. *Nature* **456:**605–610.

Fontanilla D, Johannessen M, Hajipour AR, Cozzi NV, Jackson MB, and Ruoho AE (2009) The hallucinogen N,N-dimethyltryptamine (DMT) is an endogenous sigma-1 receptor regulator. *Science* **323:**934–937.

Garmy N, Taïeb N, Yahi N, and Fantini J (2005) Apical uptake and transepithelial transport of sphingosine monomers through intact human intestinal epithelial cells: physicochemical and molecular modeling studies. *Arch Biochem Biophys* **440:**91–100.

Gebreselassie D and Bowen WD (2004) Sigma-2 receptors are specifically localized to lipid rafts in rat liver membranes. *Eur J Pharmacol* **493:**19–28.

Hajnóczky G, Csordás G, Das S, Garcia-Perez C, Saotome M, Sinha Roy S, and Yi M (2006) Mitochondrial calcium signalling and cell death: approaches for assessing the role of mitochondrial Ca^{2+} uptake in apoptosis. *Cell Calcium* **40:**553–560.

Hanner M, Moebius FF, Flandorfer A, Knaus HG, Striessnig J, Kempner E, and Glossmann H (1996) Purification, molecular cloning, and expression of the mammalian sigma1-binding site. *Proc Natl Acad Sci USA* **93:**8072–8077.

Hayashi T, Rizzuto R, Hajnoczky G, and Su TP (2009) MAM: more than just a housekeeper. *Trends Cell Biol* **19:**81–88.

Hayashi T and Su TP (2003a) Intracellular dynamics of sigma-1 receptors (sigma(1) binding sites) in NG108–15 cells. *J Pharmacol Exp Ther* **306:**726–733.

Hayashi T and Su TP (2003b) Sigma-1 receptors (sigma(1) binding sites) form raft-like microdomains and target lipid droplets on the endoplasmic reticulum: roles in endoplasmic reticulum lipid compartmentalization and export. *J Pharmacol Exp Ther* **306:**718–725.

Hayashi T and Su TP (2004) Sigma-1 receptors at galactosylceramide-enriched lipid microdomains regulate oligodendrocyte differentiation. *Proc Natl Acad Sci USA* **101:**14949–14954.

Hayashi T and Su TP (2007) Sigma-1 receptor chaperones at the ER-mitochondrion interface regulate Ca^{2+} signaling and cell survival. *Cell* **131:**596–610.

Hayashi T and Su TP (2008) An update on the development of drugs for neuropsychiatric disorders: focusing on the sigma 1 receptor ligand. *Expert Opin Ther Targets* **12:**45–58.

Herrera Y, Katnik C, Rodriguez JD, Hall AA, Willing A, Pennypacker KR, and Cuevas J (2008) sigma-1 receptor modulation of acid-sensing ion channel a (ASIC1a) and ASIC1a-induced Ca^{2+} influx in rat cortical neurons. *J Pharmacol Exp Ther* **327:**491–502.

Jacobson K, Mouritsen OG, and Anderson RG (2007) Lipid rafts: at a crossroad between cell biology and physics. *Nat Cell Biol* **9:**7–14.

Lipsky NG and Pagano RE (1983) Sphingolipid metabolism in cultured fibroblasts: microscopic and biochemical studies employing a fluorescent ceramide analogue. *Proc Natl Acad Sci USA* **80:**2608–2612.

Marwali MR, Rey-Ladino J, Dreolini L, Shaw D, and Takei F (2003) Membrane cholesterol regulates LFA-1 function and lipid raft heterogeneity. *Blood* **102:**215–222.

Matsumoto RR, Liu Y, Lerner M, Howard EW, and Brackett DJ (2003) Sigma receptors: potential medications development target for anti-cocaine agents. *Eur J Pharmacol* **469:**1–12.

Maurice T, Martin-Fardon R, Romieu P, and Matsumoto RR (2002) Sigma(1) (sigma(1)) receptor antagonists represent a new strategy against cocaine addiction and toxicity. *Neurosci Biobehav Rev* **26:**499–527.

McCann DJ and Su TP (1991) Solubilization and characterization of haloperidol-sensitive (+)-[^{3}H]SKF-10,047 binding sites (sigma sites) from rat liver membranes. *J Pharmacol Exp Ther* **257:**547–554.

Mei J and Pasternak GW (2007) Modulation of brainstem opiate analgesia in the rat by sigma 1 receptors: a microinjection study. *J Pharmacol Exp Ther* **322:**1278–1285.

Naslavsky N, Shmeeda H, Friedlander G, Yanai A, Futerman AH, Barenholz Y, and Taraboulos A (1999) Sphingolipid depletion increases formation of the scrapie prion protein in neuroblastoma cells infected with prions. *J Biol Chem* **274:**20763–20771.

Nuwayhid SJ and Werling LL (2003) Sigma1 receptor agonist-mediated regulation of *N*-methyl-D-aspartate-stimulated [^{3}H]dopamine release is dependent upon protein kinase C. *J Pharmacol Exp Ther* **304:**364–369.

Pal A, Hajipour AR, Fontanilla D, Ramachandran S, Chu UB, Mavlyutov T, and Ruoho AE (2007) Identification of regions of the sigma-1 receptor ligand binding site using a novel photoprobe. *Mol Pharmacol* **72:**921–933.

Palmer CP, Mahen R, Schnell E, Djamgoz MB, and Aydar E (2007) Sigma-1 receptors bind cholesterol and remodel lipid rafts in breast cancer cell lines. *Cancer Res* **67:**11166–11175.

Pani B, Ong HL, Liu X, Rauser K, Ambudkar IS, and Singh BB (2008) Lipid rafts determine clustering of STIM1 in endoplasmic reticulum-plasma membrane junctions and regulation of store-operated Ca^{2+} entry (SOCE). *J Biol Chem* **283:**17333–17340.

Ramachandran S, Chu UB, Mavlyutov TA, Pal A, Pyne S, and Ruoho AE (2009) The sigma1 receptor interacts with N-alkyl amines and endogenous sphingolipids. *Eur J Pharmacol* **609:**19–26.

Rizzuto R and Pozzan T (2006) Microdomains of intracellular Ca^{2+}: molecular determinants and functional consequences. *Physiol Rev* **86:**369–408.

Rusiñol AE, Cui Z, Chen MH, and Vance JE (1994) A unique mitochondria-associated membrane fraction from rat liver has a high capacity for lipid synthesis

and contains pre-Golgi secretory proteins including nascent lipoproteins. *J Biol Chem* **269:**27494–27502.
Shen H, Howles P, and Tso P.(2001) From interaction of lipidic vehicles with intestinal epithelial cell membranes to the formation and secretion of chylomicrons. *Adv Drug Deliv Rev* **50 (Suppl 1):**S103–S125.
Simons K and Toomre D (2000) Lipid rafts and signal transduction. *Nat Rev Mol Cell Biol* **1:**31–39.
Siskind LJ, Kolesnick RN, and Colombini M (2006) Ceramide forms channels in mitochondrial outer membranes at physiologically relevant concentrations. *Mitochondrion* **6:**118–125.
Snyder SH and Largent BL (1989) Receptor mechanisms in antipsychotic drug action: focus on sigma receptors. *J Neuropsychiatry Clin Neurosci* **1:**7–15.
Spiegel S and Milstien S (2003) Sphingosine-1-phosphate: an enigmatic signalling lipid. *Nat Rev Mol Cell Biol* **4:**397–407.
Sprong H, van der Sluijs P, and van Meer G (2001) How proteins move lipids and lipids move proteins. *Nat Rev Mol Cell Biol* **2:**504–513.
Su TP, London ED, and Jaffe JH (1988) Steroid binding at sigma receptors suggests a link between endocrine, nervous, and immune systems. *Science* **240:**219–221.
van Meer G, Wolthoorn J, and Degroote S (2003) The fate and function of glycosphingolipid glucosylceramide. *Philos Trans R Soc Lond B Biol Sci* **358:**869–873.

Address correspondence to: Dr. Teruo Hayashi, IRP/NIDA/NIH/DHHS, 333 Cassell Drive, Baltimore, MD 21224. E-mail: thayashi@mail.nih.gov